Phase synchronization and suppression of chaos through intermittency in forcing of an electrochemical oscillator

István Z. Kiss and John L. Hudson*
Department of Chemical Engineering, 102 Engineers' Way, University of Virginia, Charlottesville, Virginia 22904-4741
(Received 26 April 2001; published 24 September 2001)

External periodic forcing was applied to a chaotic chemical oscillator in experiments on the electrodissolution of Ni in sulfuric acid solution. The amplitude and the frequency (Ω) of the forcing signal were varied in a region around $\Omega = \omega_0$, where ω_0 is the frequency of the unforced signal. Phase synchronization occurred with increase in the amplitude of the forcing. For Ω/ω_0 near 1 the signal remained chaotic after the transition to the phase-locked state; for Ω/ω_0 somewhat farther from 1 the transition was to a periodic state via intermittency. The experimental results are supported by numerical simulations using a general model for electrochemical oscillations.

DOI: 10.1103/PhysRevE.64.046215 PACS number(s): 05.45.Xt, 82.40.Bj

I. INTRODUCTION

Synchronization in dynamical systems has received considerable interest in various fields of science involving physical, chemical, and biological systems. Several types of synchronization have been investigated including complete [1–3], phase [4], lag [5], and generalized [6] synchronization and they can be treated in a unified framework [7].

Periodic forcing of a chaotic system is a type of unidirectional coupling that can produce phase synchronization [8]. For phase synchronization only the locking of the phases of the chaotic and driving signals is significant, while no restriction on the amplitudes is imposed. The determination of the phase (and amplitude) of a chaotic system is nontrivial [9,10]; nevertheless, the different approaches allow the description of phase-locking phenomena in a reasonable way. Phase synchronization can be defined [9] as the appearance of a certain relation between the phase of a system and that of an external force, while the amplitude can remain chaotic. Phase synchronization has been experimentally verified in electronic circuits [11–14], lasers [15–17], plasma discharge [18], and biological systems [19,20].

The study of chaotic systems under the action of a weak forcing signal has also been motivated by the development of resonant chaos control methods [21] or parametric destochastization [22,23]; the chaos is suppressed by a small harmonic perturbation of a parameter. Transitions from chaotic to periodic behavior are often realized via intermittency (type I [24] or type II [25]). Parametric destochastization was experimentally observed, e.g., in lasers [26–28], discharge plasma [29], a periodically driven pendulum [30], a microwave driven spin-wave system [31], a magnetoelastic beam experiment [32], and a homogeneous chemical reaction [33].

Several electrochemical systems give rise to periodic current oscillations under potentiostatic control [34]. Harmonic forcing of periodic electrochemical oscillators resulted in transitions to chaos [35], entrainment, spike generation, and quasiperiodicity [36,37], harmonic, subharmonic, and superharmonic entrainment [38]. The chaotic electrodissolution of copper was suppressed by periodic modulation of the circuit potential, and period-1 and period-2 oscillations were observed [39].

In this paper we present experimental results on the effects of periodic forcing of a chaotic chemical oscillator, the electrodissolution of Ni in sulfuric acid solution. The dynamics of the system are investigated over a range of forcing frequency and amplitude of the applied potential. The phase of the chaotic current is compared to that of the forcing. Phase synchronization is shown to occur at low amplitudes of forcing. At higher amplitudes the transition through intermittency from chaotic to periodic motion is analyzed. The experimental findings are supported by numerical studies using a general electrochemical model.

II. EXPERIMENTAL SETUP

A standard electrochemical cell consisting of a nickel working electrode (Aldrich, 99.99%+, 2 mm diameter), a $Hg/Hg_2SO_4/K_2SO_4$ reference electrode, and a platinum mesh counterelectrode was used. The electrode is embedded in epoxy and reaction takes place only at the end. The electrode is held at the applied potential $[V_{app}(t)]$ with a potentiostat (EG&G PAR 273). The applied potential is the sum of a constant potential (V_0) and a perturbation $[\delta V(t) = A \sin 2\pi\Omega t]$ due to forcing. In all the experiments reported here $V_0 = 1.300$ V (vs $Hg/Hg_2SO_4/K_2SO_4$). The forcing signal was obtained from a HP-33120A function generator. A zero resistance ammeter was used to measure the current of the electrode and data acquisition was done at 200 Hz. Experiments were carried out in 4.5M H_2SO_4 solution at a temperature of 11 °C. The reproducibility of the experiment was greatly enhanced by slowly stirring the solution with a magnetic stirrer resulting in the continuous removal of some O_2 formed during the experiments. Before each experiment the electrode was polished with a series of emery paper and polarized at $V = 1.270$ V (region of periodic oscillations) to provide a reproducible surface film (initial condition) for the system.

*Author to whom correspondence should be addressed. Email address: hudson@virginia.edu

 ©2001 The American Physical Society

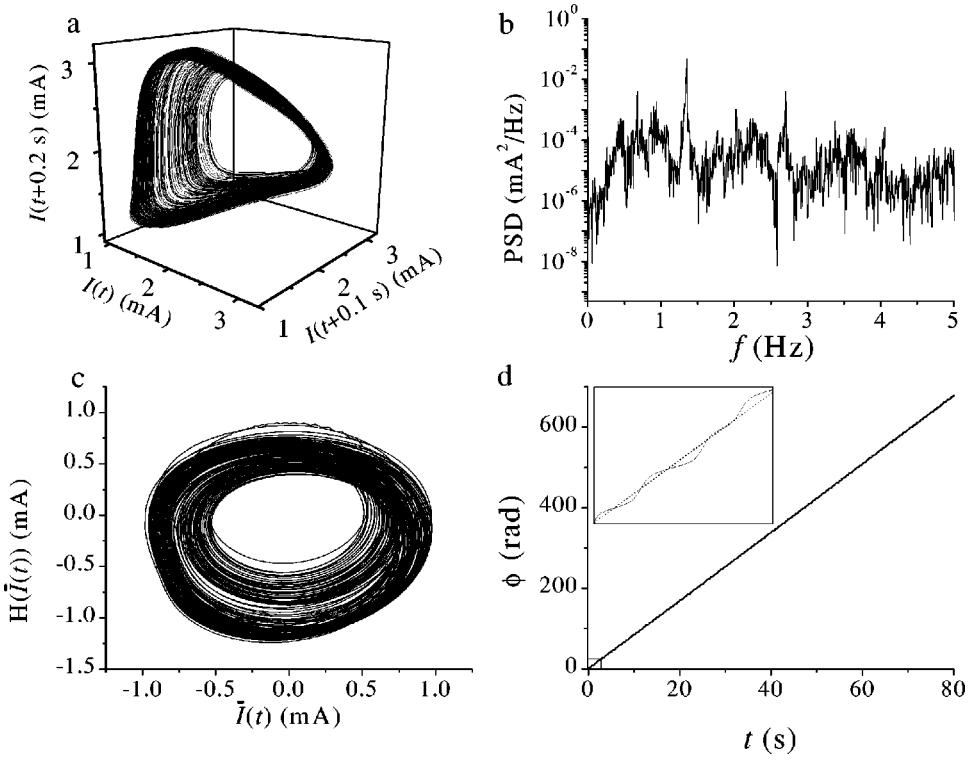

FIG. 1. Chaotic oscillator without forcing. (a) Reconstructed attractor using time delay coordinates. (b) Power spectrum. (c) Hilbert transform of the conditioned current $H(\bar{I}(t))$ vs conditioned current $\bar{I}(t)$. (d) Phase $\phi(t)$ (solid) as a function of t. The linear least-squares fit (dotted in the inset, enlarged by a factor of 32) gives the frequency of the chaotic oscillation, $\omega_0 = 1.325$ Hz.

III. EXPERIMENTAL RESULTS

A. Unforced chaotic oscillator

As reported in previous studies [40,41] the potentiostatic dissolution of Ni exhibits chaotic dynamics if an appropriate series resistance (R_s) is added to the circuit. The reconstructed chaotic attractor from the current time series data along with the corresponding power spectrum of the unforced system with $R_s = 170\,\Omega$ are shown in Figs. 1(a) and 1(b), respectively.

The chaotic attractor is low dimensional; the information dimension is 2.2 [40]. The presence of a sharp peak at $f = 1.323$ Hz in the power spectrum implies strong phase coherence indicating the possibility of phase synchronization [8].

B. Phase of the unforced system

We applied the analytical signal approach introduced by Gábor [42] to define the instantaneous phase $\phi(t)$ and amplitude $a(t)$ for the current time series data $I(t)$ (other methods are also available; see [9] for details). The analytical signal $\zeta(t)$ is a complex function of time defined as

$$\zeta(t) = I(t) + jH(I(t)) = a(t)e^{j\phi(t)}, \tag{1}$$

where

$$H(I(t)) = \pi^{-1}\int_{-\infty}^{\infty}\frac{I(\tau)}{t-\tau}d\tau \tag{2}$$

is the Hilbert transform of $I(t)$. With the phase $\phi(t)$ known from Eq. (1) the frequency (ω) of the chaotic signal is obtained as

$$\omega = \left\langle \frac{d\phi}{dt} \right\rangle. \tag{3}$$

A fundamental requirement in the implementation of this phase definition is the proper rotation of the analytical signal $\zeta(t)$, that is, there should be a definite direction (either clockwise or counterclockwise) and a unique center of rotation. To meet this requirement the scalar can be decomposed into a small number of modes of proper rotation, and the phase of the original signal is a vector quantity corresponding to the phases of the different modes [43]. We applied the following simplified version of the technique: two smooth splines connecting all maxima and minima of the current $I(t)$, respectively, were constructed and their average was subtracted from the original signal. The resulting signal is the first mode $\bar{I}(t)$, while the subtracted signal is the second mode of the original signal. The $H(\bar{I}(t))$ vs $\bar{I}(t)$ plot in Fig. 1(c) reveals that the first mode has proper rotation. The frequency of the chaotic oscillations (ω_0) obtained from the linear least-squares fit to $\phi(t)$ is $\omega_0 = 1.325$ Hz [see Fig. 1(d)]. Note that although ϕ is monotonically increasing there are some slight deviations from the fitted line [Fig. 1(d), inset]. The deviations arise because the instantaneous frequency $[d\phi(t)/dt]$ depends in general on the amplitude. Theoretical analysis of this deviation can be found in the review by Pikovsky *et al.* [9].

The second mode of the current possessed an amplitude of 5% or less at a frequency about half that of the first mode. Therefore, we neglect the low-frequency, low-amplitude second mode and study the phase synchronization of the first mode of the experimental signal. The conditioning procedure makes the phase analysis more robust against noise and some

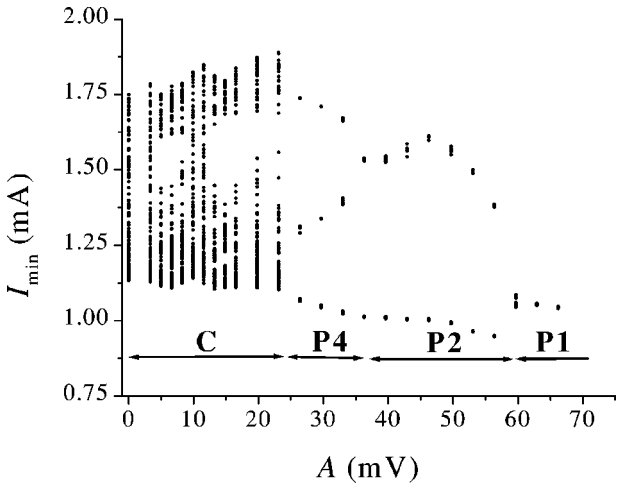

FIG. 2. Bifurcation diagram of the forced system showing the minima of the oscillations (I_{min}) as a function of the amplitude of the forcing (A). The forcing frequency $\Omega = 1.32$ Hz is within the experimental error of ω_0. The chaotic (C), period-4 (P4), period-2 (P2), and period-1 (P1) regions are also shown.

unavoidable low-frequency variations while keeping the phase information of the original signal.

During the experiments the frequency of the unforced system was repeatedly calculated and was found to be $\omega_0 = 1.33 \pm 0.015$ Hz. This deviation is probably due to experimental error, e.g., slow modification of the surface or O_2 evolution.

C. Forcing with $\Omega = \omega_0$

For forcing experiments the phases of the chaotic $[\phi(t)]$ and the periodic driving $[\psi(t)]$ signals were determined. Phase synchronization is defined [9] as the phase locking of the signal and forcing:

$$|n\phi(t) - m\psi(t)| < \text{const}, \tag{4}$$

where n and m are integers. A weaker condition can also be given (often referred to as frequency locking)

$$\omega = \frac{m}{n}\Omega, \tag{5}$$

where Ω is the frequency of the forcing. In this paper we only have $n = m = 1$ since $\Omega/\omega \cong 1$.

Results are first presented with a forcing frequency of $\Omega = 1.32$ Hz, which is within the experimental error of ω_0. A bifurcation diagram showing the minima of the oscillations as a function of the forcing amplitude is presented in Fig. 2.

At small amplitude the frequency of the oscillations locks on Ω although the chaotic dynamics are only slightly affected. Even at small amplitudes the small variation of ω (± 0.015 Hz) that had been observed in the unforced system diminishes to ± 0.001 Hz. Therefore all the dynamical states shown in Fig. 2 have exactly the same frequency regardless of the characteristics of the state. With increasing amplitude, chaos$\rightarrow$P4$\rightarrow$P2$\rightarrow$P1 transitions are observed. Note that the lowest branch of the P4 oscillations is actually two points; the values of those two minima are indistinguishable because of noise. The P4$\rightarrow$P2 and P2$\rightarrow$P1 transitions are inverse period-doubling bifurcations. The experimental data cannot reveal the nature of the chaos$\rightarrow$P4 transition. One possible scenario might be an experimentally not resolvable period-doubling sequence. However, we cannot exclude the possibility of intermittency, which was observed with $\Omega \neq \omega_0$ (see later).

D. Forcing with $\Omega \neq \omega_0$

When the forcing frequency is different from ω_0 phase locking occurs only for $A \geqslant A_c$, where A_c is the critical amplitude of the forcing signal. The phase difference $\Delta\phi(t) = \phi(t) - \psi(t)$ between the chaotic oscillations and the driving signal is shown in Fig. 3 with increasing A for $\Omega = 1.37$ Hz, i.e., slightly higher than ω_0.

At $A = 3.3$ mV [Fig. 3(a)] the forcing is too weak to affect the phase characteristics of the chaotic behavior significantly; $\Delta\phi$ decreases almost linearly with increasing t. Increasing A to 6.0 mV [Fig. 3(b)] still does not result in phase synchronization; however, $\Delta\phi(t)$ exhibits a steplike variation consisting of almost horizontal phase-locked regions and vertical phase slips. The phenomenon of phase slipping has been observed and analyzed [44,45]. Increasing A further to 7.3 mV [Fig. 3(c)] results in a state very close to phase synchronization: during the experiment only one phase slip occurs. At $A = 8.6$ mV [Fig. 3(d)] phase synchronization takes place: the chaotic signal takes on the frequency of the forcing ($\omega = \Omega$) and the oscillations have an approximately fixed, nonzero ($\Delta\phi \cong 2$) phase difference. The phase synchronized chaotic attractor shown in Fig. 4 resembles the unforced one [Fig. 1(a)].

Some aspects of phase synchronization can also be seen in the power spectrum (insets in Fig. 3). In the forced systems a new peak emerges close to $f_{max} = 1.32$ Hz corresponding to the frequency of the driving signal, $\Omega = 1.37$ Hz. With increasing A the new peak increases, and at phase synchronization [Fig. 3(d)] only this peak corresponding to the forcing can be seen.

Forcing experiments have been carried out for a range of forcing frequencies between 1.21 Hz and 1.45 Hz. The $\Omega - \omega$ vs Ω plots are presented in Fig. 5.

At $A = 0$ [without forcing, Fig. 5(a)] the points lie approximately on a line with a slope of unity; deviations are due to the small variations of ω_0. For a small amplitude [$A = 6.6$ mV, Fig. 5(b)] phase synchronization occurs only for frequencies close to ω_0. As the amplitude is made larger, the phase synchronized frequency region increases as can be seen in Figs. 5(c) and 5(d). At the smallest ($\Omega = 1.21$ Hz) and the largest ($\Omega = 1.45$ Hz) frequencies phase synchronization occurs at larger values of forcing amplitude ($A \cong 25$ mV). Figure 6 shows the critical forcing amplitude A_c at which phase synchronization is observed.

This figure is analogous to the phase diagram of the forced periodic oscillators showing the ''Arnold tongues'' of frequency-locked regions [46,47]. The experimentally determined synchronization tongue is approximately symmetric around ω_0.

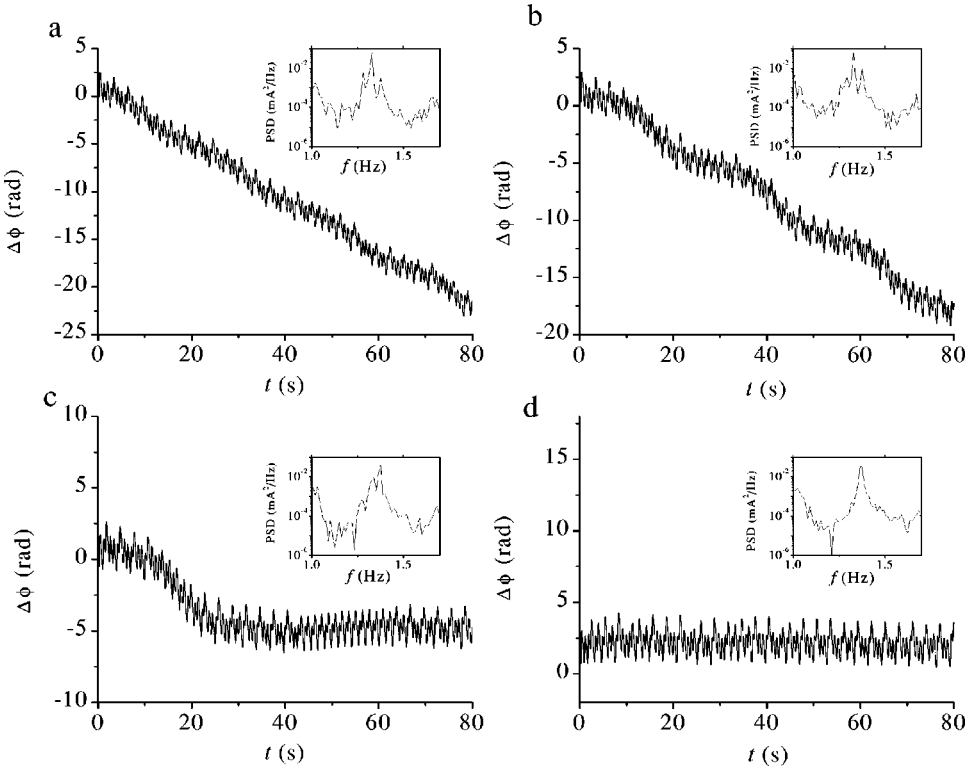

FIG. 3. The phase difference ($\Delta\phi$) between the chaotic signal and the forcing for $\Omega=1.37$ Hz. (a) $A=3.3$ mV. (b) $A=6.0$ mV. (c) $A=7.3$ mV. (d) $A=8.6$ mV. The corresponding power spectra are shown in the insets.

The bifurcation diagrams at the different frequencies were found to be similar to the one presented in Fig. 2 where $\Omega=\omega_0$. For 1.21 Hz$\leqslant\Omega\leqslant$1.40 Hz the transitions are chaos $\rightarrow$P4$\rightarrow$P2$\rightarrow$P1. For $\Omega=1.45$ Hz no P4 state was seen and the transitions were chaos$\rightarrow$P2$\rightarrow$P1. For larger forcing frequencies ($\Omega\geqslant1.40$ Hz) the transition into the phase-locked region was qualitatively different; instead of a chaotic phase synchronization there is an intermittent transition from chaos to a periodic state; the periodic state is P2 for $\Omega=1.45$ Hz and P4 for $\Omega=1.40$ Hz. The time series of the current and the phase difference are shown in Fig. 7 for $\Omega=1.45$ Hz. Figures 7(a) and 7(b) are for a forcing amplitude ($A=23.1$ mV) just below critical.

The long P2 sequence is interrupted by short chaotic one. The periodic region is phase synchronized, while during the chaotic region there is a phase slip. The current and phase difference are shown for amplitude close to the critical in Figs. 7(c) and 7(d) ($A=24.7$ mV); phase synchronization and period-2 oscillations are seen. For $\Omega=1.40$ Hz, i.e., closer to ω_0, a similar intermittent transition was observed; however, the chaotic (not phase synchronized) state was transformed to a P4 (phase synchronized) state.

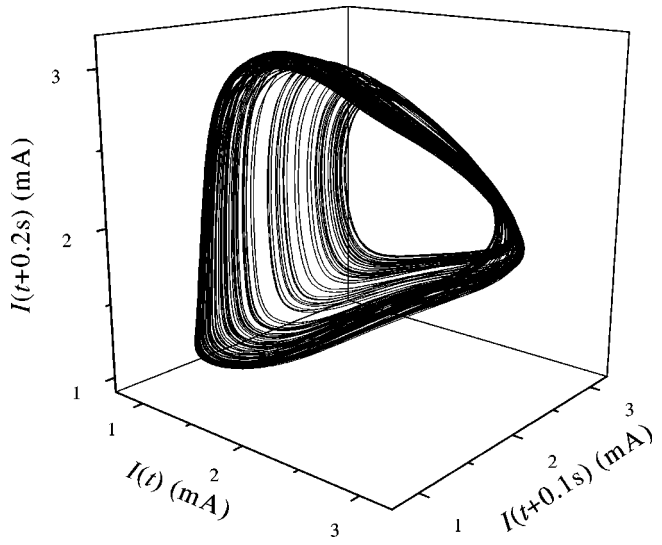

FIG. 4. The phase synchronized chaotic attractor. The experimental conditions are given in Fig. 3(d).

IV. NUMERICAL RESULTS

To support the experimental findings some numerical simulations have been carried out with a general dimensionless electrochemical oscillator model proposed by Koper and Gaspard [48]:

$$\frac{de}{dt}=\frac{V_{\mathrm{app}}-e}{R_s}-120k(e)u, \tag{6}$$

$$\frac{du}{dt}=-1.25d^{0.5}k(e)u+2d(w-u), \tag{7}$$

$$\frac{dw}{dt}=1.6d(2-3w+u), \tag{8}$$

where e is the double-layer potential, u and w are the concentrations of electroactive species in the so-called ''surface'' and ''diffusion'' layers, d is the rotation rate of the electrode characterizing the mass transfer, and $k(e)$ is defined as follows:

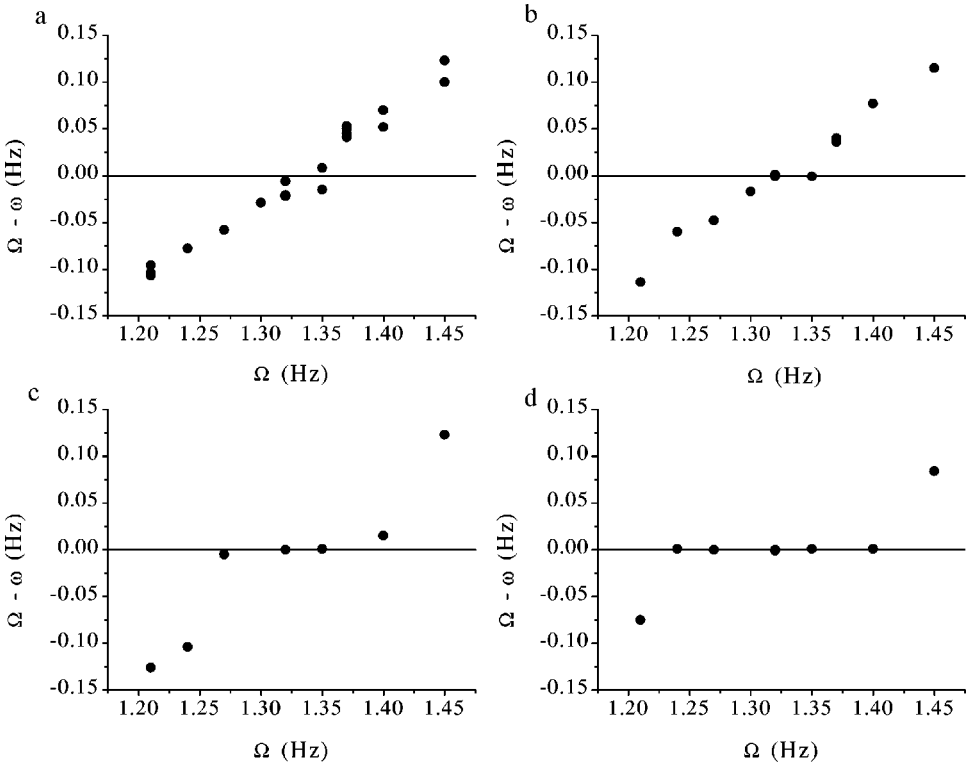

FIG. 5. The frequency difference $(\Omega-\omega)$ as a function of the forcing frequency (Ω) for (a) $A=0$ mV, (b) $A=6.6$ mV, (c) $A=13.2$ mV, and (d) $A=16.5$ mV.

$$k(e)=2.5\theta^2+0.01\exp[0.5(e-30)], \tag{9}$$

where θ is related to the surface coverage by some (inhibiting) chemical species. The value of θ is approximated by a sigmoidal function

$$\theta=\begin{cases}1 & \text{for } e\leqslant 35\\ \exp[-0.5(e-35)^2] & \text{for } e>35.\end{cases} \tag{10}$$

For an appropriate parameter set $d=0.119\,13$, $R_s=0.02$ the model exhibits a cascade of period-doubling bifurcations with increasing V_0. The chaotic attractor reconstructed from the dimensionless current, $I=(V_{app}-e)/R_s$, is shown in Fig. 8(a) at $V_0=36.7395$.

There is a sharp peak in the power spectrum [Fig. 8(b)] at $f_{max}=0.475$ Hz. We analyzed the phase of the simulated data as was done with the experiments except that no conditioning was required. The frequency of the chaotic oscillations was found to be $\omega_0=0.475$, the same as f_{max}. The effect of periodic forcing $[V_{app}(t)=V_0+\sin 2\pi\Omega t,\ V_0=36.7395]$ on the dynamics is shown in Fig. 8(c) with $\Omega=\omega_0$. The bifurcation diagram is qualitatively similar to that obtained in the experiments in the low-forcing-amplitude region $(A<5\times10^{-4})$ in which the phase synchronization occurs. Above this period-2 region the behavior is more complicated than that for the experiments but eventually doesgive period-1 oscillations through a series of periodic and chaotic states. Here we study phase synchronization in the low-amplitude-forcing region where there is qualitative agreement between experiment and simulation.

Chaotic phase synchronization is shown in Fig. 8(d) at $\Omega=0.471$. With increasing A phase slips occur more often until complete phase synchronization takes place at $A_c=2.4\times10^{-5}$. Note that the phase difference is not zero during phase synchronization but rather has a finite value as in the experimental findings.

The phase synchronized region in the A vs Ω parameter space is shown in Fig. 9. In the frequency range of $0.470\leqslant\Omega\leqslant0.479$ the tongue is symmetric (inset) around $\omega_0=0.475$, while out of the region some asymmetry develops. In the symmetric range chaotic phase synchronization takes place. Outside this range destochastization occurs via an intermittent phase synchronization. For $\Omega<0.470$, chaos $\rightarrow$P2 $(0.41\leqslant\Omega\leqslant0.460)$ and chaos$\rightarrow$P4 transitions $(\Omega=0.465)$ occur. Similar transitions were found in the experi-

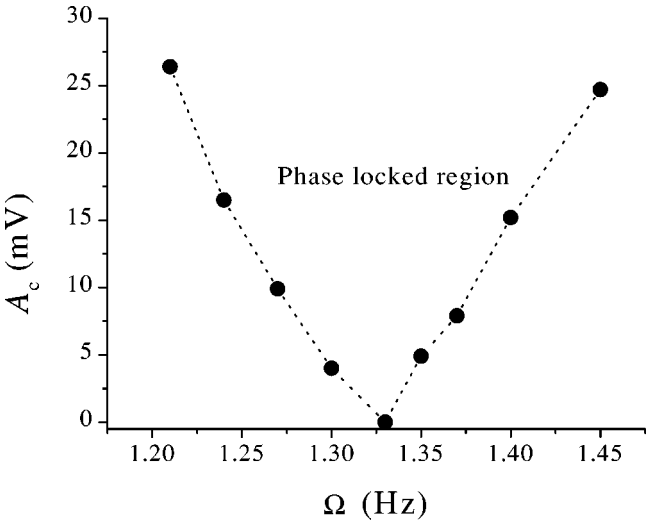

FIG. 6. The phase-locked region in A-Ω parameter space.

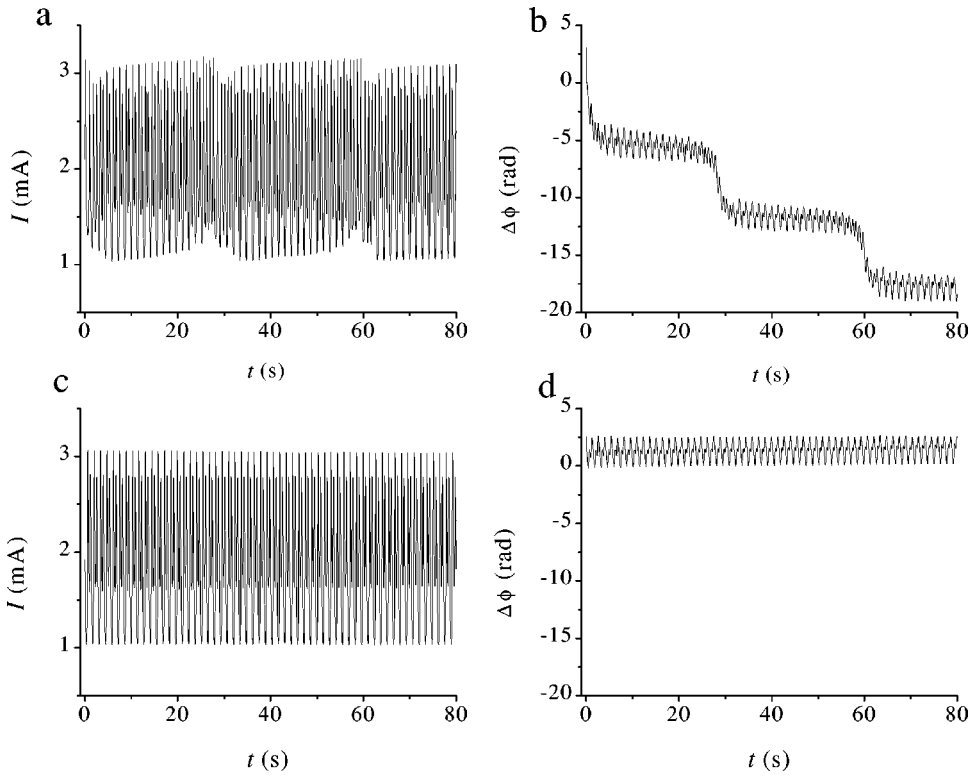

FIG. 7. Current time series and phase differences, $\Omega = 1.45$ Hz. (a,b) Intermittent periodic and chaotic oscillations with phase slips. $A = 23.1$ mV, $A < A_{\mathrm{crit}}$. (c,d) Phase synchronized period state, $A = 24.7$.

ments. For $\Omega > 0.479$ transitions from chaos to P3, from chaos to P2, and from chaos to P1 took place at the critical amplitude where phase synchronization occurs.

In Fig. 10 the chaos→P2 transition is shown for $\Omega = 0.450$. At $A = 2.0 \times 10^{-4}$ the long intermittent P2 sequence is interrupted by chaotic phase slips. With increasing A the average length $\langle \tau \rangle$ of the phase synchronized periodic regions (laminar phases) increases. It was found that $\langle \tau \rangle \propto (A_c - A)^{-0.46}$ indicating type-I intermittency and a saddle-node bifurcation of periodic orbits [49] at $A_c = 2.015 \times 10^{-4}$. Above A_c, e.g., at $A = 2.2 \times 10^{-4}$ [Figs. 10(c) and 10(d)], phase synchronized P2 behavior occurs.

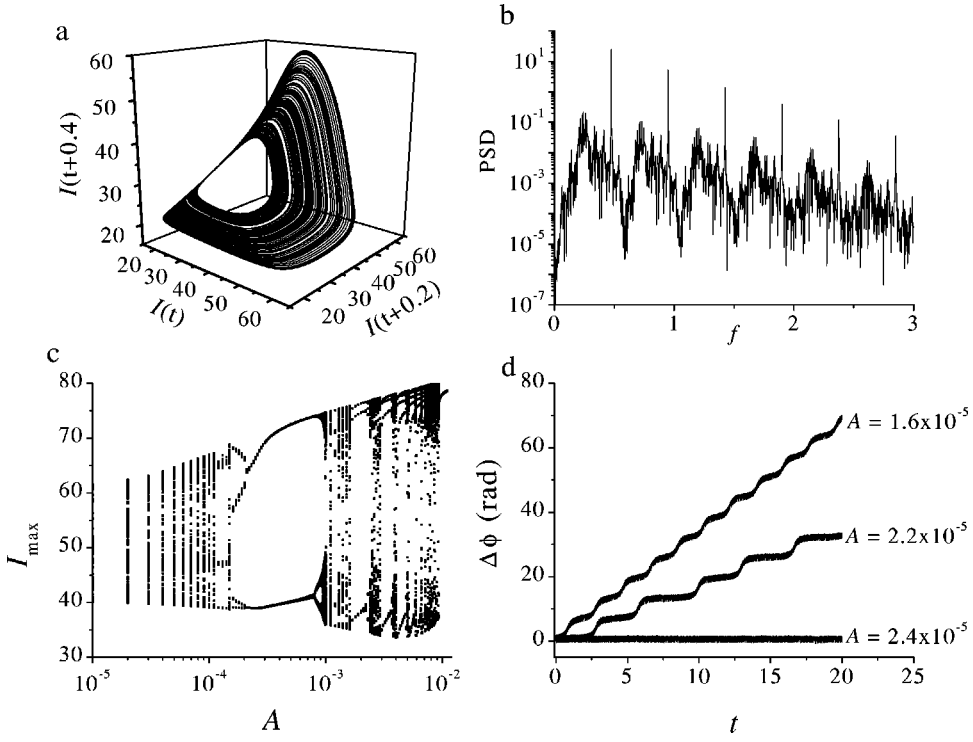

FIG. 8. Numerical simulations. (a) The unforced chaotic attractor. (b) The corresponding power spectrum. (c) The bifurcation diagram of the forced system ($\Omega = 0.475$) showing the maxima of the oscillations (I_{max}) as a function of the forcing amplitude (A). (d) The phase difference between the current and the forcing signal ($\Omega = 0.471$) as a function of time with increasing amplitude (shown next to the curves).

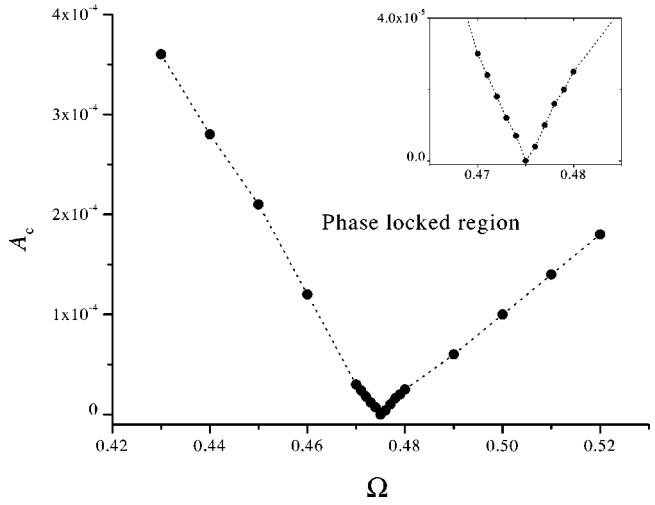

FIG. 9. Numerical simulation. The phase-locked region of the forced model in the forcing frequency (Ω) – forcing amplitude (A) parameter space. The inset shows the magnified region around the frequency of the unforced system ($\omega_0 = 0.475$).

V. DISCUSSION

Phase synchronization was experimentally observed during periodic forcing of the chaotic electrodissolution of Ni in sulfuric acid solution. Unsynchronized, intermittently synchronized (with phase slips), and phase synchronized states were observed with increases in the forcing amplitude. In the phase synchronized region the phases are locked with non-zero phase difference. Phase differences can occur in electrochemistry due to double-layer charging (capacitive impedance) and transport effects (Warburg impedance) [50]. These are routinely investigated with periodic forcing of a steady state (impedance spectroscopy).

The bifurcations responsible for phase synchronization of chaotic oscillators have been described theoretically [44]; the role of phase locking of the unstable periodic orbits embedded in the chaotic attractor was emphasized. Phase locking of periodic oscillators is known to take place through saddle-node bifurcations of periodic orbits [46,47]. In our experiments when the forcing frequency was sufficiently removed from ω_0 an intermittent transition took place resulting in a periodic phase synchronized state. The phase synchronized P2 (P4) state goes through an inverse period-doubling bifurcation (sequence) resulting in a phase-locked P1 state.

We have carried out numerical simulations of a model of a forced chaotic electrochemical oscillator to support the experimental findings. Although the model captures only some general features of an electrochemical oscillator, it was found to be capable of describing the chaotic phase synchronization and the intermittent transitions from chaotic to periodic behaviors. Numerical calculations imply type-I intermittency, i.e., stable and unstable periodic orbits emerge through a saddle-node bifurcation. A related behavior was observed in a driven Rayleigh oscillator [24]. Since the model provides a general mechanism for electrochemical oscillators it is probable that similar transitions can be observed in other electrochemical systems having a phase coherent chaotic attractor. Such systems are the reduction of indium (III) ions on hanging mercury electrode [51] the electrodis-

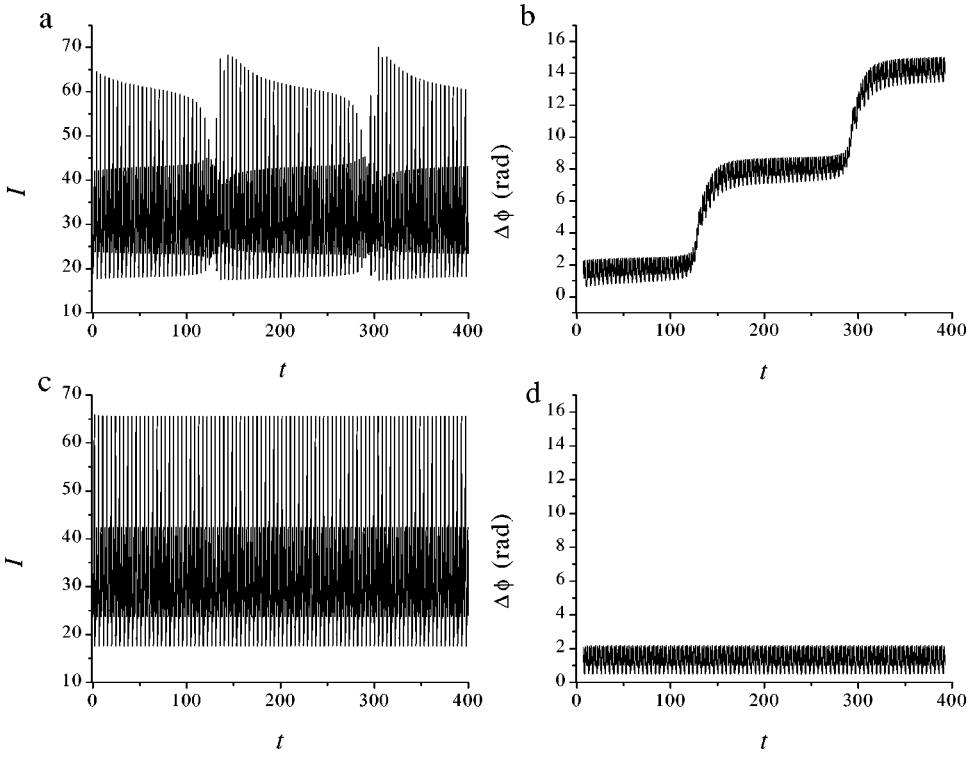

FIG. 10. Current time series and phase differences from numerical simulation ($\Omega = 1.45$ Hz). (a,b). Intermittent periodic and chaotic oscillations with phase slips. $A = 2.0 \times 10^{-4}$, $A < A_{\mathrm{crit}}$. (c,d) Phase synchronized period state, $A = 2.2 \times 10^{-4}$.

solution of copper in phosphoric acid [52] and acetic acid electrolytes [53].

The observed rich dynamics makes the system also suitable for studying the effect of forcing on a population of chaotic oscillators [54]. In this case the forcing, by changing dynamics of the individual elements, alters the collective dynamics, and stable and intermittent clustering have been shown to occur [55].

ACKNOWLEDGMENTS

This work was supported by the National Science Foundation and the Office of Naval Research.

[1] L.M. Pecora and T.L. Carroll, Phys. Rev. Lett. **64**, 821 (1990).
[2] H. Fujisaka and T. Yamada, Prog. Theor. Phys. **69**, 32 (1983).
[3] A.S. Pikovsky and P. Grassberger, J. Phys. A **24**, 4587 (1991).
[4] M.G. Rosenblum, A.S. Pikovsky, and J. Kurths, Phys. Rev. Lett. **76**, 1804 (1996).
[5] M.G. Rosenblum, A.S. Pikovsky, and J. Kurths, Phys. Rev. Lett. **78**, 4193 (1997).
[6] N.F. Rulkov, M.M. Sushchik, L.S. Tsimring, and H.D.I. Abarbanel, Phys. Rev. E **51**, 980 (1995).
[7] R. Brown and L. Kocarev, Chaos **10**, 344 (2000).
[8] E.F. Stone, Phys. Lett. A **163**, 367 (1992).
[9] A.S. Pikovsky, M.G. Rosenblum, G.V. Osipov, and J. Kurths, Physica D **104**, 219 (1997).
[10] A. S. Pikovsky, M. G. Rosenblum, M. A. Zaks, and J. Kurths, in *Handbook of Chaos Control*, edited by H. G. Schuster (Wiley-VCH, Weinheim, 1999).
[11] U. Parlitz, L. Junge, W. Lauterborn, and L. Kocarev, Phys. Rev. E **54**, 2115 (1996).
[12] M.G. Rosenblum, A.S. Pikovsky, and J. Kurths, IEEE Trans. Circuits Syst., I: Fundam. Theory Appl. **44**, 874 (1997).
[13] N.F. Rulkov and M.M. Sushchik, Phys. Lett. A **214**, 145 (1996).
[14] N.F. Rulkov, Chaos **6**, 262 (1996).
[15] D.Y. Tang, R. Dykstra, M.W. Hamilton, and N.R. Heckenberg, Chaos **8**, 697 (1998).
[16] D.Y. Tang, R. Dykstra, M.W. Hamilton, and N.R. Heckenberg, Phys. Rev. E **57**, 5247 (1998).
[17] P.M. Varangis, A. Gavrielides, T. Erneux, V. Kovanis, and L.F. Lester, Phys. Rev. Lett. **78**, 2353 (1997).
[18] C.M. Ticos, E. Rosa, W.B. Pardo, J.A. Walkenstein, and M. Monti, Phys. Rev. Lett. **85**, 2929 (2000).
[19] A. Neiman, X. Pei, D. Russell, W. Wojtenek, L. Wilkens, F. Moss, H.A. Braun, M.T. Huber, and K. Voigt, Phys. Rev. Lett. **82**, 660 (1999).
[20] C. Schafer, M.G. Rosenblum, J. Kurths, and H.H. Abel, Nature (London) **392**, 239 (1998).
[21] R. Lima and M. Pettini, Phys. Rev. A **41**, 726 (1990).
[22] A.Y. Loskutov, J. Phys. A **26**, 4581 (1993).
[23] V.V. Alexeev and A.Y. Loskutov, Sov. Phys. Dokl. **32**, 270 (1987).
[24] T. Tamura, N. Inaba, and J. Miyamichi, Phys. Rev. Lett. **83**, 3824 (1999).
[25] R. Chacón, Phys. Rev. E **51**, 761 (1995).
[26] P. Colet and Y. Braiman, Phys. Rev. E **53**, 200 (1996).
[27] D. Dangoisse, J.C. Celet, and P. Glorieux, Phys. Rev. E **56**, 1396 (1997).
[28] R. Meucci, W. Gadomski, M. Ciofini, and F.T. Arecchi, Phys. Rev. E **49**, R2528 (1994).
[29] W.X. Ding, H.Q. She, W. Huang, and C.X. Yu, Phys. Rev. Lett. **72**, 96 (1994).
[30] Y. Braiman and I. Goldhirsch, Phys. Rev. Lett. **66**, 2545 (1991).
[31] A. Azevedo and S.M. Rezende, Phys. Rev. Lett. **66**, 1342 (1991).
[32] L. Fronzoni, M. Giocondo, and M. Pettini, Phys. Rev. A **43**, 6483 (1991).
[33] A. Guderian, A.F. Münster, M. Jinguji, M. Kraus, and F.W. Schneider, Chem. Phys. Lett. **312**, 440 (1999).
[34] J.L. Hudson and T.T. Tsotsis, Chem. Eng. Sci. **49**, 1493 (1994).
[35] V.S. Varma and P.K. Upadhyay, J. Electroanal. Chem. **271**, 345 (1989).
[36] A. Karantonis, M. Pagitsas, and D. Sazou, Chaos **3**, 243 (1993).
[37] M. Pagitsas, D. Sazou, A. Karantonis, and C. Georgolios, J. Electroanal. Chem. **327**, 93 (1992).
[38] M. Pagitsas and D. Sazou, J. Electroanal. Chem. **386**, 89 (1995).
[39] P. Parmananda, M. Rivera, R. Madrigal, I.Z. Kiss, and V. Gáspár, J. Phys. Chem. B **104**, 11 748 (2000).
[40] I.Z. Kiss, W. Wang, and J.L. Hudson, Phys. Chem. Chem. Phys. **2**, 3847 (2000).
[41] O. Lev, A. Wolffberg, M. Sheintuch, and L.M. Pismen, Chem. Eng. Sci. **43**, 1339 (1988).
[42] D. Gábor, J. Inst. Electr. Eng., Part 3 **93**, 429 (1946).
[43] T. Yalçinkaya and Y.C. Lai, Phys. Rev. Lett. **79**, 3885 (1997).
[44] A. Pikovsky, M. Zaks, M. Rosenblum, G. Osipov, and J. Kurths, Chaos **7**, 680 (1997).
[45] E. Rosa, E. Ott, and M.H. Hess, Phys. Rev. Lett. **80**, 1642 (1998).
[46] V.I. Arnold, Am. Math. Soc. Transl. Ser. 2; **46**, 213 (1965).
[47] E. Ott, *Chaos in Dynamical Systems* (Cambridge University Press, Cambridge, 1993).
[48] M.T.M. Koper and P. Gaspard, J. Chem. Phys. **96**, 7797 (1992).
[49] P. Manneville and Y. Pomeau, Physica D **1**, 219 (1980).
[50] A.J. Bard and L.R. Faulkner, *Electrochemical Methods: Fundamentals and Applications* (John Wiley & Sons, New York, 1980).
[51] M.T.M. Koper and J.H. Sluyters, J. Electroanal. Chem. **303**, 65 (1991).
[52] M. Schell and F.N. Albahadily, J. Chem. Phys. **90**, 822 (1989).
[53] H.D. Dewald, P. Parmananda, and R.W. Rollins, J. Electrochem. Soc. **140**, 1969 (1993).
[54] W. Wang, I.Z. Kiss, and J.L. Hudson, Chaos **10**, 248 (2000).
[55] W. Wang, I.Z. Kiss, and J.L. Hudson, Phys. Rev. Lett. **86**, 4959 (2001).